

Probing ^{27}Al – ^{13}C proximities in metal–organic frameworks using dynamic nuclear polarization enhanced NMR spectroscopy†

Cite this: *Chem. Commun.*, 2014, 50, 933

Received 20th September 2013,
Accepted 14th November 2013

DOI: 10.1039/c3cc47208f

www.rsc.org/chemcomm

Frédérique Pourpoint,^a Aany Sofia Lilly Thankamony,^a Christophe Volklinger,^a Thierry Loiseau,^a Julien Trébosc,^a Fabien Aussenac,^b Diego Carnevale,^c Geoffrey Bodenhausen,^{cd} Hervé Vezin,^e Olivier Lafon^{*a} and Jean-Paul Amoureux^{af}

We show how ^{27}Al – ^{13}C proximities in the microporous metal–organic framework MIL-100(Al) can be probed using advanced ^{27}Al – ^{13}C NMR methods boosted by Dynamic Nuclear Polarization.

Metal–organic frameworks (MOFs) have attracted increasing attention owing to their high surface area and their wide range of three-dimensional (3D) architectures that exhibit different pore apertures and chemical tunabilities. These hybrid materials represent promising systems for gas storage, catalysis, capture of radioactive compounds, and drug delivery.¹ Amongst them, aluminium-based MOFs, such as MIL-100(Al),² present many advantages, including low cost, density and toxicity, remarkable thermal stability and high Lewis acidity that should allow many industrial applications.³

Rational design of MOFs requires a clear understanding of structure–property relationships and hence calls for characterization methods endowed with atomic resolution. In particular, solid-state NMR is well suited to assess structural models of MOF frameworks, to probe the organization of extra-framework entities,⁴ and to analyze atomic-level dynamics.^{5,6} However, the poor sensitivity of NMR limits the observation of adsorbed species, defects, *etc.*, particularly when the observed nuclei have low gyromagnetic ratios, low natural abundances or long longitudinal relaxation times (T_1). Besides, the observation of ^{27}Al – ^{13}C proximities by NMR in Al-based MOFs has hitherto been hindered by limitations of common NMR

probes, which cannot be tuned simultaneously to nearby ^{27}Al and ^{13}C Larmor frequencies.

We report here the first observation of ^{27}Al – ^{13}C proximities in MOFs using advanced NMR methods combined with a frequency splitter.^{7,8} We show that Dynamic Nuclear Polarization (DNP) can significantly reduce acquisition times for MIL-100(Al) at 100 K. EPR spectroscopy and DNP enhancements prove that the biradical TOTAPOL⁹ enters the MIL-100(Al) cavities within tens of minutes, although its apertures are smaller than 0.88 nm. Besides, DNP-enhanced ^{27}Al – ^{13}C correlation experiments prove that the MIL-100(Al) framework is not altered by impregnation with a TOTAPOL solution. So far, DNP of MOFs has only been demonstrated for 1D spectra under Magic-Angle Spinning (MAS) using $^1\text{H} \rightarrow ^{13}\text{C}$ and $^1\text{H} \rightarrow ^{15}\text{N}$ cross-polarisation (CP) and 2D ^1H – ^{13}C correlation spectroscopy of In-based MIL-68.¹⁰ So far, ^{27}Al DNP has only been reported for γ - and mesoporous alumina.¹¹

Fig. 1d shows the EPR spectra of MIL-100(Al) impregnated with a 16 mM aqueous TOTAPOL solution (1). Immediately after impregnation the EPR spectrum is dominated by a triplet due to the isotropic hyperfine coupling with ^{14}N . During impregnation, an additional triplet develops mono-exponentially with a time constant of 77 min (Fig. 1f), which is consistent with the kinetics of the adsorption of organic molecules on MIL-100 from aqueous solutions.¹² This triplet is due to the anisotropic hyperfine coupling with ^{14}N and corresponds to TOTAPOL adsorbed on MIL-100(Al). So far, EPR has never been used to probe adsorption of radicals onto MOFs.

Fig. 1e and g show 1D $^1\text{H} \rightarrow ^{13}\text{C}$ and $^1\text{H} \rightarrow ^{27}\text{Al}$ CP-MAS spectra of 1 with and without microwave (μw) irradiation (Fig. S2a and b, ESI†). Three ^{13}C signals are resolved, which can be assigned to three sites of the benzene-1,3,5-tricarboxylate (btc) moiety, based on the ^{13}C chemical shifts of btc in solution and 2D ^{27}Al – ^{13}C spectra (see below). The $^1\text{H} \rightarrow ^{27}\text{Al}$ CP-MAS spectra are similar to the directly detected ^{27}Al signals of hydrated MIL-100(Al), with overlapping signals of octahedral Al sites.¹³ Fig. 1e and g show DNP enhancements per scan, $\epsilon_{\text{on/off}}^{\text{scan}} \approx 8.5$, which are identical for all ^{13}C and ^{27}Al sites. A similar enhancement is measured for the ^1H polarization under MAS (Fig. S3, ESI†), which is the source of the ^{27}Al and ^{13}C polarization when using CP. The radicals do not

^a Université Lille Nord de France, CNRS, UMR 8181 UCCS, ENSCL, Université de Lille 1, 59652 Villeneuve d'Ascq, France. E-mail: frederique.pourpoint@enscl-lille.fr, olivier.lafon@univ-lille1.fr; Tel: +33 320436542

^b Bruker BioSpin SA, 34, rue de l'Industrie, 67166 Wissembourg Cedex, France

^c Institut des sciences et ingénierie chimiques, Ecole Polytechnique Fédérale de Lausanne, EPFL, Batochime, CH-1015 Lausanne, Switzerland

^d Département de chimie, Ecole Normale Supérieure, 24, rue Lhomond, 75321 Paris cedex 05, France

^e Université Lille Nord de France, CNRS, UMR LASIR 8516, Université de Lille 1, 59652 Villeneuve d'Ascq, France

^f East China Normal University, Shanghai, China

† Electronic supplementary information (ESI) available: Experimental section, additional DNP and standard NMR data, spin dynamics simulations and a discussion of DNP enhancement values. See DOI: 10.1039/c3cc47208f

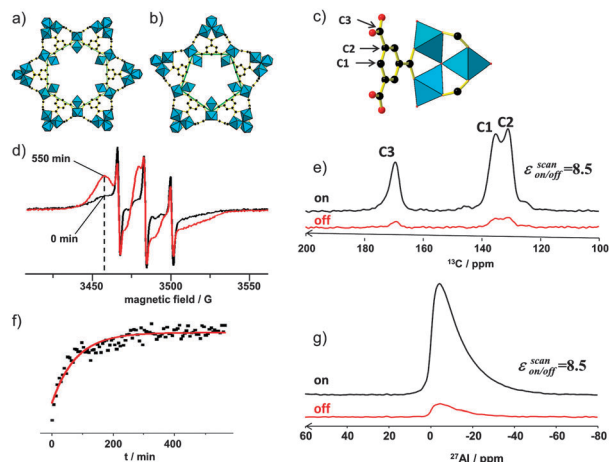


Fig. 1 Representations of the (a) hexagonal and (b) pentagonal apertures of MIL-100(Al) (Fig. S1, ESI†). (c) Representation of the btc moiety attached to Al trimers. (d) 9 GHz continuous wave EPR spectra of **1** at room temperature after an impregnation time of 0 (black) and 550 min (red). (f) Evolution of experimental EPR intensity (square symbols) at 3458 G (dashed line in d) for **1** as a function of impregnation time. The continuous line is the best mono-exponential fit. (e) ^{13}C MAS NMR spectra of **1** at 100 K with CP from ^1H at $B_0 = 9.4$ T with (black) and without (red) μw irradiation, using zirconia rotors spinning at $\nu_r = 10$ kHz. (g) ^{27}Al MAS NMR spectra of **1** under the same conditions with CP from ^1H .

affect the linewidths of ^{27}Al and ^{13}C CP-MAS signals.¹⁴ As for other biradicals, the build-up time of the DNP-induced ^1H polarization is equal to $T_1(^1\text{H}) = 0.7$ s, as determined without μw irradiation in the same sample.¹⁵ Hence, μw irradiation does not allow reducing the recovery delay, so that the enhancement per unit time is $\epsilon_{\text{on/off}}^{\text{time}} = \epsilon_{\text{on/off}}^{\text{scan}} \approx 8.5$. When compared to standard room-temperature CP-MAS spectra of dry MIL-100(Al), DNP-CP-MAS at 100 K provides a global sensitivity enhancement of $\epsilon_{\text{global}}^{\text{time}} = 10$.¹⁶

The TOTAPOL molecule is approximately 1.2 nm long and 0.65 nm wide. Hence, it can enter the large cavities of MIL-100(Al) through the hexagonal apertures of 0.88 nm (Fig. 1a), but not the small cavities with pentagonal apertures of 0.54 nm (Fig. 1b). The TOTAPOL diffusion into MIL-100(Al) is confirmed by EPR and by a quantitative analysis of the DNP enhancement using a ^1H spin diffusion model for spherical samples (see ESI†).

The significant enhancement of $\epsilon_{\text{on/off}}^{\text{scan}} \approx 13$ for direct ^{13}C polarization (with MAS but without resorting to CP) corroborates the presence of TOTAPOL in the pores of MIL-100(Al) (Fig. S4a, ESI†). The (integrated) intensities of the ^{13}C signals exhibit a stretched exponential DNP build-up where the longest time constant is a few hundreds of seconds (Fig. S6, ESI†).¹⁴ Polarization build-up curves are identical with and without μw and $\epsilon_{\text{on/off}}^{\text{time}} = \epsilon_{\text{on/off}}^{\text{scan}}$ do not depend on the recovery delay. However, ^{13}C linewidths obtained by direct DNP-MAS (without CP) with short recycle delays are twice broader than with DNP-CP-MAS (Fig. S5a, ESI†),¹⁴ since direct DNP transfer emphasizes ^{13}C nuclei that are close to TOTAPOL. In this sample, the sensitivity of $^1\text{H} \rightarrow ^{13}\text{C}$ DNP-CP-MAS is approximately equal to direct ^{13}C DNP-MAS without CP. The disadvantage of direct polarization compared to CP-MAS is compensated by DNP. On the other hand, losses due to paramagnetic $T_{1\rho}$ relaxation during CP partly cancel sensitivity gains resulting from CP from remote

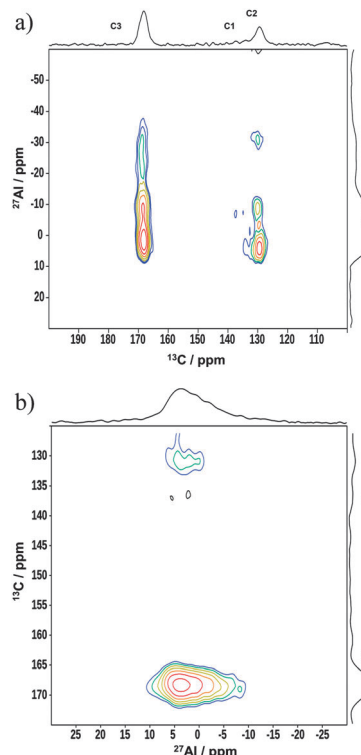


Fig. 2 DNP-enhanced (a) $^{13}\text{C}\{-^{27}\text{Al}\}$ CP-D-HMQC 2D spectra of **1** and (b) $^{27}\text{Al}\{-^{13}\text{C}\}$ at $B_0 = 9.4$ T, $\nu_r = 10$ kHz and $T = 100$ K. Additional details are given in the ESI.†

protons relayed by ^1H spin diffusion.¹⁶ The enhancement $\epsilon_{\text{on/off}}^{\text{scan}} = 1.7$ is modest for ^{27}Al (Fig. S4b, ESI†). Besides, the direct build-up of ^{27}Al polarization occurs within a few seconds and no line broadening is observed (Fig. S5b, ESI†).

The sensitivity enhancement afforded by DNP allows one to acquire 2D NMR experiments that are precluded under standard conditions. Fig. 2 shows $^{27}\text{Al}\{-^{13}\text{C}\}$ Dipolar-mediated Heteronuclear Multiple Quantum Correlation (D-HMQC) spectra of MIL-100(Al) (Fig. S2c and d, ESI†). The acquisition of these spectra was made possible by combining a frequency splitter with DNP for sensitivity enhancement.⁷ Without DNP, no signal could be seen after three days in a D-HMQC spectrum of dry MIL-100(Al) using $^1\text{H} \rightarrow ^{13}\text{C}$ CP excitation (CP-D-HMQC) and ^{13}C detection (denoted $^{13}\text{C}\{-^{27}\text{Al}\}$ hereafter), whereas the signal-to-noise ratio (S/N) of the CP-D-HMQC spectrum with ^{27}Al detection (denoted $^{27}\text{Al}\{-^{13}\text{C}\}$) was $\text{S/N} < 2$ after 17 h (Fig. S7, ESI†). This poor sensitivity stems not only from the 1.1% natural abundance of the ^{13}C isotope but also from coherent and incoherent losses during the D-HMQC sequence. For instance, the efficiency of the $^{13}\text{C}\{-^{27}\text{Al}\}$ CP-D-HMQC spectrum relative to $^1\text{H} \rightarrow ^{13}\text{C}$ CP-MAS is about 10%. The DNP enhancement compensates for this low efficiency, and the $^{13}\text{C}\{-^{27}\text{Al}\}$ CP-D-HMQC spectrum acquired in 7.1 h exhibits a $\text{S/N} \approx 30$ for the C3 signal. Under DNP conditions, $^{13}\text{C}\{-^{27}\text{Al}\}$ CP-D-HMQC spectra are more sensitive than with ^{27}Al detection, $^{27}\text{Al}\{-^{13}\text{C}\}$, since $^1\text{H} \rightarrow ^{13}\text{C}$ CP-MAS is more efficient and easier to optimize than $^1\text{H} \rightarrow ^{27}\text{Al}$ CP-MAS. Hence, $^{13}\text{C}\{-^{27}\text{Al}\}$ CP-D-HMQC should be preferred in this case.

Such $^{27}\text{Al}\{-^{13}\text{C}\}$ correlation spectra allow one to identify $^{27}\text{Al}\{-^{13}\text{C}\}$ proximities in MIL-100(Al). In agreement with the crystal

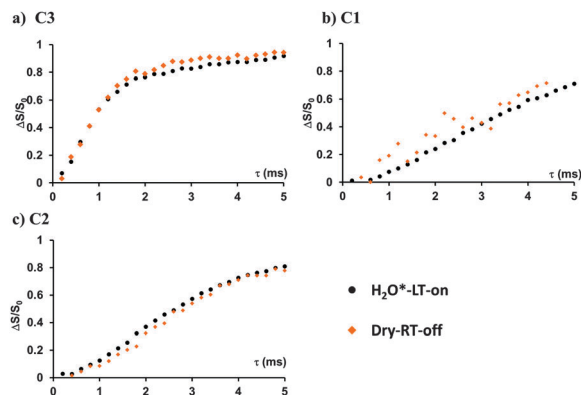


Fig. 3 Comparison of the ^{27}Al - ^{13}C S-RESPDOR curves of three ^{13}C signals of (i) **1** with microwave irradiation at 100 K (black circles, denoted $\text{H}_2\text{O}^*\text{-LT-on}$) and (ii) dry MIL-100(Al) without microwave irradiation at room temperature (orange diamonds, denoted dry-RT-off). Both experiments were recorded at 9.4 T with $\nu_r = 10$ kHz. The total experimental time was 7 and 50 h, with and without DNP, respectively. Additional experimental details are given in the ESI†

structure, C2 and C3 display cross-peaks with several octahedral Al sites. Weak C1 cross-peaks are also visible. The cross-peak intensities decrease with increasing ^{27}Al - ^{13}C distances: $I(\text{C3}) > I(\text{C2}) > I(\text{C1})$ (Table S2, ESI†), thus confirming the assignment of ^{13}C signals based on isotropic chemical shifts in solution. DNP facilitates the detection of weak cross-peaks and hence of large ^{27}Al - ^{13}C distances.

However, simple *D*-HMQC experiments are not suitable for a quantitative assessment of ^{27}Al - ^{13}C distances. This is possible using Symmetry-based Rotational-Echo Saturation-Pulse Double-Resonance (S-RESPDOR) (Fig. S2e, ESI†).⁸ However, under standard conditions, the low S/N of S-RESPDOR spectra acquired in 50 h leads to noisy dipolar dephasing curves (dry-RT-off data in Fig. 3b). DNP can help to overcome this problem, although the presence of TOTAPOL accelerates signal decay and hence decreases the efficiency of S-RESPDOR (Fig. S8, ESI†).

The DNP-S-RESPDOR curves of Fig. 3 were acquired in only 7 h. DNP is especially useful to detect slow dipolar dephasing, like for C1 and C2, which correspond to long ^{27}Al - ^{13}C distances. Furthermore, there is a good agreement between the S-RESPDOR signal fractions of MIL-100(Al) obtained by DNP-NMR and conventional NMR. This result demonstrates that the impregnation with an aqueous TOTAPOL solution and freezing to low temperature do not affect the MIL-100(Al) framework. Besides, the experimental S-RESPDOR signal fractions agree with those expected from the crystal structure of MIL-100(Al) (Fig. S9, ESI†). This agreement validates crystal structures obtained from X-ray diffraction analysis.

In summary, we demonstrated by EPR and DNP experiments that TOTAPOL can diffuse into the large cavities of microporous MIL-100(Al), leading to DNP sensitivity enhancements for CP-MAS and direct polarization ^{13}C MAS experiments. We reported the first 2D ^{27}Al - ^{13}C correlation experiments on MOFs

and showed that the time required for these experiments can be reduced using DNP. These experiments validate the crystal structure of MIL-100(Al) and the assignment of the ^{13}C resonances. Besides, S-RESPDOR experiments demonstrate that impregnation and freezing down to 100 K do not alter the MIL-100(Al) framework. Our new ^{27}Al - ^{13}C DNP-NMR methods should have implications for the characterization of other advanced materials, including alkylaluminum^{7,8} and microporous organic polymers.¹⁷ The reader is referred to ESI†

This work was supported by the Region Nord/Pas de Calais, the European Union (FEDER), the CNRS, the French ministry of research, USTL, ENSCL, contracts ANR-2020-jcjc-0811-01 and COST TD 1103, EPFL, the Swiss National Science Foundation, the Swiss Commission for Technology and Innovation, and Bruker Biospin.

Notes and references

- Reviews on MOFs: J. R. Long and O. M. Yaghi, *Chem. Soc. Rev.*, 2009, **38**, 1207; H. C. Zhou, J. R. Long and O. M. Yaghi, *Chem. Rev.*, 2012, **112**, 673.
- C. Volkringer, D. Popov, T. Loiseau, G. Férey, M. Burghammer, C. Riekel, M. Haouas and F. Taulelle, *Chem. Mater.*, 2009, **21**, 5695.
- M. Gaab, N. Trukhan, S. Maurer, R. Gummaraju and U. Muller, *Microporous Mesoporous Mater.*, 2012, **157**, 131.
- M. Haouas, C. Volkringer, T. Loiseau, G. Férey and F. Taulelle, *Chem.-Eur. J.*, 2009, **15**, 3139.
- S. Horike, R. Matsuda, D. Tanaka, S. Matsubara, M. Mizuno, K. Endo and S. Kitagawa, *Angew. Chem., Int. Ed.*, 2006, **45**, 7226; L. C. Lin, J. Kim, X. Q. Kong, E. Scott, T. M. McDonald, J. R. Long, J. A. Reimer and B. Smit, *Angew. Chem., Int. Ed.*, 2013, **52**, 4410.
- H. C. Hoffmann, M. Debowski, P. Muller, S. Paasch, I. Senkovska, S. Kaskel and E. Brunner, *Materials*, 2012, **5**, 2537; A. Sutrisno and Y. N. Huang, *Solid State Nucl. Magn. Reson.*, 2013, **49–50**, 1.
- F. Pourpoint, Y. Morin, F. Capet, J. Trébosc, R. M. Gauvin, O. Lafon and J. P. Amoureux, *J. Phys. Chem. C*, 2013, **117**, 18091.
- F. Pourpoint, J. Trébosc, R. M. Gauvin, Q. Wang, O. Lafon, F. Deng and J. P. Amoureux, *ChemPhysChem*, 2012, **13**, 3605.
- C. S. Song, K. N. Hu, C. G. Joo, T. M. Swager and R. G. Griffin, *J. Am. Chem. Soc.*, 2006, **128**, 11385.
- A. J. Rossini, A. Zagdoun, M. Lelli, J. Canivet, S. Aguado, O. Ouari, P. Tordo, M. Rosay, W. E. Maas, C. Coperet, D. Farrusseng, L. Emsley and A. Lesage, *Angew. Chem., Int. Ed.*, 2012, **51**, 123.
- D. Lee, H. Takahashi, A. S. Lilly Thankamony, J. P. Dacquin, M. Bardet, O. Lafon and G. De Paepe, *J. Am. Chem. Soc.*, 2012, **134**, 18491; V. Vitzthum, P. Mieville, D. Carnevale, M. A. Caporini, D. Gajan, C. Coperet, M. Lelli, A. Zagdoun, A. J. Rossini, A. Lesage, L. Emsley and G. Bodenhausen, *Chem. Commun.*, 2012, **48**, 1988.
- S. H. Huo and X. P. Yan, *J. Mater. Chem.*, 2012, **22**, 7449.
- M. Haouas, C. Volkringer, T. Loiseau, G. Férey and F. Taulelle, *J. Phys. Chem. C*, 2011, **115**, 17934.
- O. Lafon, A. S. Lilly Thankamony, M. Rosay, F. Aussenac, X. Lu, J. Trébosc, V. Bout-Roumazielles, H. Vezin and J. P. Amoureux, *Chem. Commun.*, 2013, **49**, 2864.
- O. Lafon, A. S. Lilly Thankamony, T. Kobayashi, D. Carnevale, V. Vitzthum, I. I. Slowing, K. Kandel, H. Vezin, J. P. Amoureux, G. Bodenhausen and M. Pruski, *J. Phys. Chem. C*, 2013, **117**, 1375.
- T. Kobayashi, O. Lafon, A. S. Lilly Thankamony, I. I. Slowing, K. Kandel, D. Carnevale, V. Vitzthum, H. Vezin, J. P. Amoureux, G. Bodenhausen and M. Pruski, *Phys. Chem. Chem. Phys.*, 2013, **15**, 5553.
- Y. Xie, T.-T. Wang, X.-H. Liu, K. Zou and W.-Q. Deng, *Nat. Commun.*, 2013, **4**, 1960; F. Blanc, S. Y. Chong, T. O. McDonald, D. J. Adams, S. Pawsey, M. A. Caporini and A. J. Cooper, *J. Am. Chem. Soc.*, 2013, **135**, 15290.